Soil microstructure as an under-explored feature of biological soil crust hydrological properties: Case study from the NW Negev Desert

Article in Biodiversity and Conservation · April 2014

DOI: 10.1007/s10531-014-0693-7

Biodivers Conserv
DOI 10.1007/s10531-014-0693-7

ORIGINAL PAPER

Soil microstructure as an under-explored feature of biological soil crust hydrological properties: case study from the NW Negev Desert

Vincent John Martin Noah Linus Felde · Stephan Peth · Daniel Uteau-Puschmann · Sylvie Drahorad · Peter Felix-Henningsen

Received: 15 November 2013 / Revised: 19 March 2014 / Accepted: 3 April 2014

Abstract Biological soil crusts (BSCs) can play an important role in hydrological cycles, especially in dryland ecosystems where the availability of water is limited. Many factors influence the hydrological behavior of BSCs, one of which is the microstructure. In order to describe the influence of the soil microstructure of BSCs on water redistribution, we investigated the change of the pore system of three different successional stages of BSCs, as well as their respective subcrusts in the NW Negev desert, Israel, using 2-dimensional thin sections, as well as non-invasive X-ray 3D computed microtomography (XCMT) and mercury intrusion porosimetry. Our results show that the pore system undergoes significant changes during crust succession. Both the total porosity, as well as the pore sizes significantly increased from cyano- to lichen- to mosscrust and the pore geometry changed from tortuous to straight pore shapes. We introduce two new mechanisms that contribute to the hydrological properties of the BSCs in the NW Negev that impede infiltration: (i) vesicular pores and (ii) a discontinuous pore system with capillary barrier effects, caused by a rapid change of grain sizes due to sand burial. Since both of these mechanisms are present mostly in early stage cyanobacterial crusts and their abundance decreases strongly with succession, it is very likely that they influence BSC hydrology to different extents in the various crust types and that they are partly responsible for differences in runoff in the NW Negev.

Communicated by Guest Editors of S.I.: Biocrust.

V. J. M. N. L. Felde · S. Drahorad · P. Felix-Henningsen
Institute of Soil Science and Soil Conservation, Justus Liebig University Giessen, Giessen, Germany

V. J. M. N. L. Felde (✉)
Institut für Bodenkunde und Bodenerhaltung, Heinrich-Buff-Ring 26-32, 35392 Giessen, Germany
e-mail: Vincent.Felde@umwelt.uni-giessen.de

S. Peth · D. Uteau-Puschmann
Department of Soil Science, University of Kassel, Kassel, Germany

Published online: 13 April 2014

Keywords Biological soil crust · Capillary barrier · Computed tomography · Soil microstructure · Pore size distribution · Vesicular pores

Introduction

Biological soil crusts (BSCs) may consist of cyanobacteria, algae, fungi, bacteria, lichen and mosses that adhere to soil particles and are a common feature of land surfaces around the world. They are often called ecosystem engineers because they are a key factor of many matter fluxes in their particular ecosystems. They influence the C and N cycles through N-fixation, photosynthetic activity and dust capture (Belnap 2002; Delgado-Baquerizo et al. 2013; Drahorad et al. 2013; Verrecchia et al. 1995), affect the emergence and vitality of both annual and perennial plants (Berkeley et al. 2005; Hernandez and Sandquist 2011; Prasse and Bornkamm 2000; Su et al. 2009) and create favorable habitats for soil fauna (Darby et al. 2010; Liu et al. 2011). Especially in arid and semiarid ecosystems, where water is scarce and usually restricted to a given season, the most important effect on the ecosystem might be the modification of hydrological processes by changing infiltration properties and thereby generating runoff, which ultimately determines many of the aforementioned functions (Chamizo et al. 2012; Kidron et al. 2012; Yair et al. 2011).

BSC hydrology

When investigating the hydrological behavior of BSCs, many different factors must be taken into account, such as texture (Rossi et al. 2012), hydrophobicity and absorptivity of biotic and abiotic crust components (Lichner et al. 2013), properties of the pore system (Verrecchia et al. 1995), surface roughness (influencing runoff path connectivity and the surface area available for infiltration) (Rodríguez-Caballero et al. 2012) or association with physical crusts (Malam Issa et al. 2011). The complex interactions between these variables may be responsible for contradictory findings regarding the influence of BSCs in hydrological cycles. These have been reviewed by Belnap (2006). Here, we focus on a case study in the NW Negev, Israel. Previous research in the NW Negev has found that the number of runoff events during a rainy season and the amount of runoff yield decreases linearly with increasing annual rainfall along a steep rainfall gradient (see Fig. 1a) (Almog and Yair 2007; Yair et al. 2011). Even though this phenomenon seems counterintuitive, it becomes logical when it is attributed to the change of surface properties, namely the succession of the BSCs and the change of their attributes along the rainfall gradient. The surface roughness, crust thickness and the content of fines all increase, resulting in a significantly higher field capacity (Yair et al. 2011). This means that the thicker BSC in the northern areas can absorb much of the rain during low intensity rainfall events, while the thinner crust in the southern areas is saturated much faster and then able to initiate surface runoff (Almog and Yair 2007). When hydrophobicity is absent, as it has been reported to be the case in the Negev (Kidron et al. 2010), the initiation of runoff is often also attributed to pore clogging following the swelling of crust components (Fischer et al. 2010; Kidron et al. 1999; Kidron et al. 2012), which reduces the effective pore space available for water movement. The clogging of pores has been reported to be a fast process. Kidron et al. (1999) found that the effect of pore clogging starts after 6 min of sprinkling experiments in the laboratory. Fischer et al. (2010) also detected a decrease of steady state water flow during infiltration experiments on BSCs in NE Germany only 5 min after wetting, which continued to decrease until the end of the experiment after 30 min. Nevertheless, when looking at rainfall patterns of the NW Negev, it is obvious that not only what happens 5 min after initiation of rain is relevant for water redistribution in the ecosystem, but also water movement during the very beginning of a rain event. Kidron and Yair (1997) reported that 70 % of the rainstorms recorded in the NW Negev between 1990 and 1994 had rain amounts of below 5 mm and that their intensities seldom exceeded 12 mm h^{-1}. Water balance studies in the NW Negev, based on TDR measurements showed that rainfall events up to 5 mm do not contribute to the water balance of the soil up to a depth of 120 cm, due to interception by the crust (Rummel and Felix-Henningsen 2004). Furthermore, Yair et al. (2011) estimated the time required for runoff generation to be as low as 1–2 min for most rain events. We therefore hypothesize that the initial infiltration properties of the BSCs are of much greater importance for most of the rain events than the infiltration properties 5 or 10 min after wetting. These initial infiltration properties are determined by the structural properties of the crust and, in particular, by the existence of a secondary pore system, which strongly promotes rain water infiltration through the crust.

BSC structure

In many studies about BSCs, no distinction is made between the different crust layers but, instead, the crust is treated as one single entity. This is, however, inadequate when looking at matter fluxes in the crust. Therefore, following an approach of Yair (1990), we differentiated between the active layer of the topcrust (TC), which is usually ~2 mm thick, and the inactive subcrust (SC) that can be several cm thick (Fig. 2a, c). TC and SC differ strongly in many parameters, such as stability (which is the main reason for the chosen subdivision), the content of fines and carbonates, amount and composition of soil organic matter, pH and salt content (Drahorad and Felix-Henningsen 2012; Drahorad and Felix-Henningsen 2013; Drahorad et al. 2013; Felix-Henningsen et al. 2008). In contrast to a BSC, which develops on a pre-existing physical crust (structural or erosional, cf. Malam Issa et al. 2011), the SC from the NW Negev evolves only after the stabilization of the dune sands through BSCs. One mechanism of SC formation is the precipitation of soluble salts and carbonates at the contact points of the sand grains during drying, thereby cementing them (Felix-Henningsen et al. 2008). Another is the reestablishment of a BSC over an old BSC, which was buried during a sandstorm (Drahorad and Felix-Henningsen 2013, see Fig. 2b, d). The role that can be played by an underlying SC in hydrological processes was described by Malam Issa et al. (2011), who found that runoff on BSCs in Niger differs significantly depending on the nature of their particular SC. In addition to the first physical discontinuity at the soil surface, caused by higher silt, clay and organic matter of the BSC (Coppola et al. 2011), the SC represents a second small-scale discontinuity in the soil profile, only that it is within the crust itself. Since the stability of the crust sections was the reason for the chosen division in the field (TC/SC), it is clear that this separation does not adequately describe the complex microstructure of the BSC, especially when considering different successional stages. Over the past decade, many studies have been published about the general microstructure of BSCs. For BSCs in the Gurbantunggut Desert, China, Zhang et al. (2006) described a fine layer of eolian material on top of an organic layer with filamentous cyanobacteria, but no SC. Mager (2010) refers to an active crust at 0–5 mm and an inorganic layer below 5 mm in the Kalahari Desert, South Africa. Williams et al. (2012) described two layers that can be separated at the macro scale. The first layer was termed the bio–rich zone that is highly cohesive and varies in thickness from

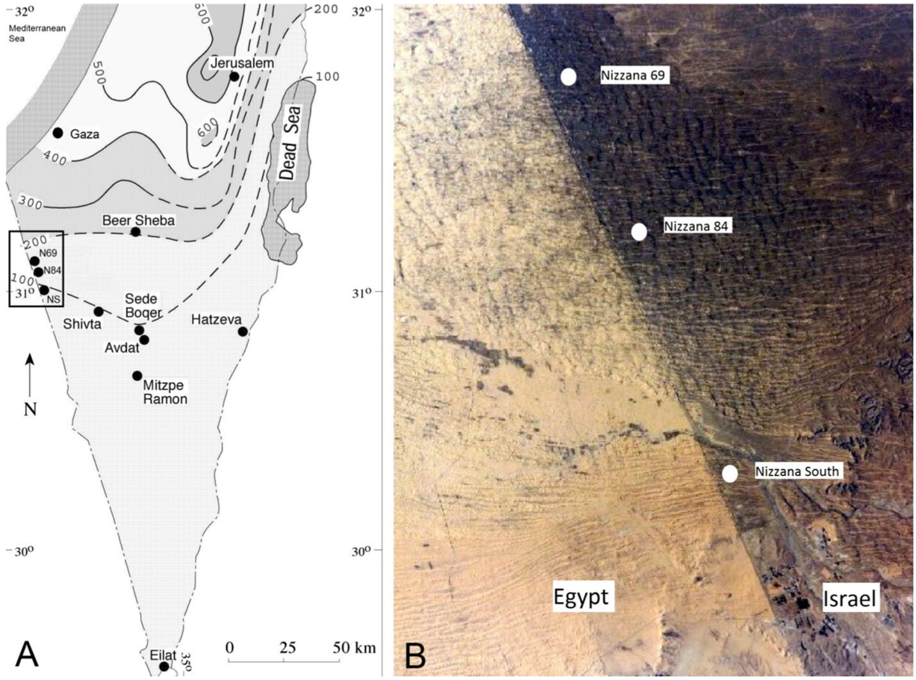

Fig. 1 **a** Rainfall map of southern Israel and Gaza Strip with isohyets showing average annual rainfall (mm) (after Israel Meteorological Service) and study sites in the NW Negev (*box*). **b** Location of the study sites along the border between Israel and Egypt. *Darker surface color* on the Israeli side is due to undisturbed biological soil crust cover (satellite image from NASA, taken on June, 3 2002)

0.5 to 22 mm. The second layer was termed the bio-poor zone, which is non-cohesive because it consists mainly of poorly consolidated sand. In BSCs in Nevada, USA, these two layers are commonly separated by a linear void. This linear void was also confirmed by Miralles-Mellado et al. (2011) for BSCs from the Tabernas Desert, SE Spain (especially for lichen crusts). For BSCs in Niger, Malam Issa et al. (2009) also described an active top layer that had an increased content of fines and was underlain by a SC consisting of ancient BSCs that had been buried by sediment. Moreover, for BSCs of the SE Tengger Desert, China, the vertical stratification varied depending on crust successional stage. Hu et al. (2003) and Lan et al. (2012) reported that initial algae crusts show an inorganic surface layer with no or few algae from 0 to 0.02 mm (similar to the one described by Zhang et al. 2006). This layer is followed by an algae-dense layer at depth 0.02–1 mm and an algae-sparse layer underneath it at depth 1–5 mm. The stronger developed, lichendominated crusts show a thallus layer, up to 1 mm above the soil surface, a rhizoid layer from 0 to 1 to 3 mm and a sub-rhizoid layer from 3 to 7 mm. Finally, the moss crusts are characterized by stem-leaf layer, which stands 2 mm above the soil surface, a rhizoid layer from 0 to 2 to 6 mm depth and a sub-rhizoid layer at depth 6–15 mm.

Naturally, both total porosity and pore size distribution (PSD) are important parameters when evaluating the hydrological behavior of a soil. For example, the importance of the radius of a pore for laminar flow becomes very clear when one uses the Hagen–Poiseuille equation, where pore radius is considered in the fourth power. This means that a reduction of the pore radius by 50 % causes an increase of the drag forces by 16 times. Nevertheless,

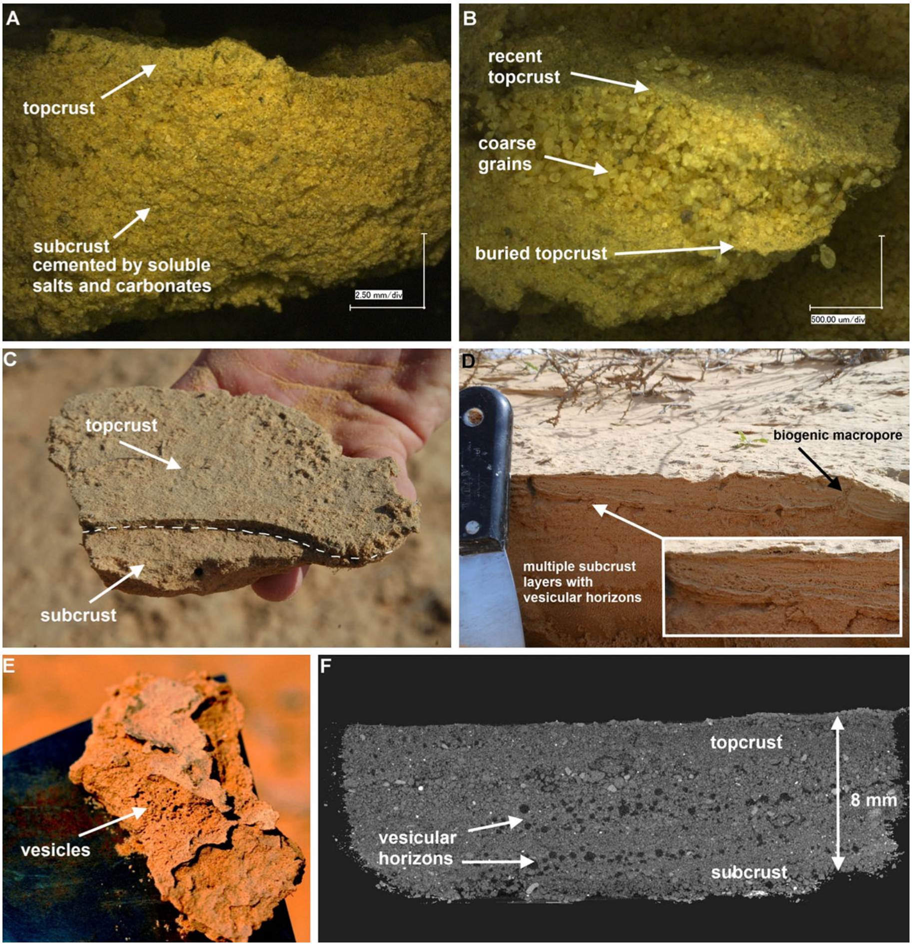

Fig. 2 Two different kinds of subcrust from a cyanobacterial crust. **a** Mineral subcrust that is created when salts and carbonates cement the sand grains together at the contact points. **b** Relict subcrust that consists of an old topcrust, which was buried by coarse sand grains during a sand storm. Subsequently the crust organisms migrated to the new surface, creating a new topcrust. **c** *Dotted line* denotes the border between the thin cyanobacterial topcrust and the massive subcrust, which is stabilized only by salts and carbonates. **d** Multiple layers of relic topcrusts, forming the new subcrust. Insert shows two vesicular horizons between the former topcrusts. **e** Vesicular pores under the topcrust of a cyanocrust in Nizzana south. **f** Two consecutive vesicular horizons in a computed tomography cross section of a cyanobacterial crust

when considering hydraulic conductivity, the shape and continuity of the pore system might be of much greater importance (Valentin and Bresson 1992). Here we present a better way to investigate these parameters by means of non-destructive, 3D X-ray computed microtomography.

Biological soil crusts and X-ray computed microtomography (XCMT)

The technique of XCMT offers a very sophisticated, non-invasive way to investigate the inner structure of an undisturbed soil sample in three dimensions and is very well suited to study fragile BSC samples. Although the use of computed tomography is increasingly common in soil science (as reviewed in Taina et al. 2008), to the best of our knowledge there are only two reports to date using this technique to study BSC structure. Menon et al. (2011) used CT-techniques to characterize the change of the inner structure of cyanobacterial and cyanobacterial-lichenous BSC after disturbance and found that both mechanical disturbance, as well as crust type had a significant impact on the porosity. Coppola et al. (2011) compared the structure of BSCs of different ages with the loose sand underneath it and found differences in pore geometry and porosity, but did not explicitly distinguish between successional stages or a TC and SC.

Aim of the study

Data about changes to the pore system during crust succession, as well as between TC and SC, are scarce but very important for understanding the hydrological phenomenon (i.e. infiltration and runoff) reported upon in the NW Negev by Yair et al. (2011). The aim of this study is therefore to compare the microstructure and properties of the pore system of three different BSC types and their respective SCs in the NW Negev in order to better understand their hydrological behavior.

Materials and methods

Study sites

The study area is located in the NW Negev, Israel, and lies directly along the border between Israel and Egypt (see Fig. 1a). This sand dune ecosystem falls within a steep rainfall gradient, running from the Gaza Strip on the Mediterranean coastline (app. 350 mm) to the Nizzana region (app. 100 mm). Rainfall occurs mainly between December and February (Littmann and Berkowicz 2008). This rapid change in annual rainfall has a crucial impact on the ecosystem in general and on the BSCs that exist here. The area can be subdivided into two different dune systems, the Haluza Agur and the Sde Hallamish sands, which are separated by the Wadi Lavan. The cessation of land use for grazing or agriculture occurred in 1982 following the peace treaty between Israel and Egypt. The absence of further disturbance led to the colonization of BSCs on the formerly mobile dunes (Tsoar 2008), stabilizing them and protecting them from wind erosion (Belnap and Gillette 1998) and consequently from further movement on the Israeli side (Fig. 1b). The three study sites established along this gradient are (from south to north) Nizzana South (NS), Nizzana 84 (N84) and Nizzana 69 (N69), which have approximately 100, 130 and 170 mm of annual rainfall, respectively (cf. also Yair et al. 2011). The distance between the northernmost and the southernmost site is $\sim$20 km. The Nizzana South site is situated within the Hebrew University of Jerusalem Arid Ecosystems Research Center (AERC) field station. The other 2 sites along the rainfall gradient are in small stations that the AERC established for monitoring.

Sampling

Representative samples from the interdune of each of the three sites were taken at the beginning of the dry season in 2011 by pushing a petri dish gently into the soil and cutting the BSC with a spatula (Fig. 3). The samples were taken in the interspace between the perennial shrubs in five repetitions. Apart from small spots with local disturbance, the BSC cover on the weakly developed Arenosols of the interdune was almost 100 % in the interspace. The three successional stages of BSCs (cyanocrust: CC, lichencrust: LC and mosscrust: MC) that were sampled are comparable to the three crust types described by Almog and Yair (2007). The species composition of the different BSCs in the NW Negev was reviewed by Büdel and Veste (2008).

Mercury intrusion porosimetry (MIP)

Pore size distribution of the dry TC and SC samples was measured using a Hg–porosimeter Autopore III (Micromeritics Instruments Corporation, Norcross, USA) at the Karlsruhe Institute of Technology (KIT), Karlsruhe, Germany. We measured 19 samples in total ($N = 2$–4 for each type). The contact angle and surface tension between BSC and mercury were 130° and 0.485 N m^{-1}, while the operating pressure ranged from 0.003 to 306 MPa. Similar to the analysis of particle size distribution by sedimentation, where non-spherical particles are treated as spherical particles via the concept of equivalent diameter, pore sizes measured with MIP are not of one shape only, but should be understood and used as the equivalent diameter of cylindrical pores (Webb and Orr 1997). For reasons of clarity, we chose to use both cumulative, as well as differential intrusion curves to illustrate MIP results (Ferreiro et al. 2010, Webb and Orr 1997). As the results of Verrecchia et al. (1995) and our own data show, the percentage of pores under 1 μm in the Negev BSCs, is negligible. These small pores play only a minor role in soil hydrology and are not present in any of the crusts we investigated. It was therefore decided to neglect pores <1 μm and show only pores within the range of 1000–1 μm.

XCMT

The three crust samples were scanned with a Phoenix Nanotom (GE Sensing & Inspection Technologies GmbH, Wunstorf, Germany) at the Institute of Plant Nutrition and Soil Science of the University of Kiel, Germany. Maximum X-ray energy during scanning was 150 keV and 1440 projections for a single rotation were acquired. The resulting voxel edge length was 5.5 μm. The technique of X-ray imaging is based on the fact that the X-ray beam experiences a decrease of its initial intensity while moving through an object which

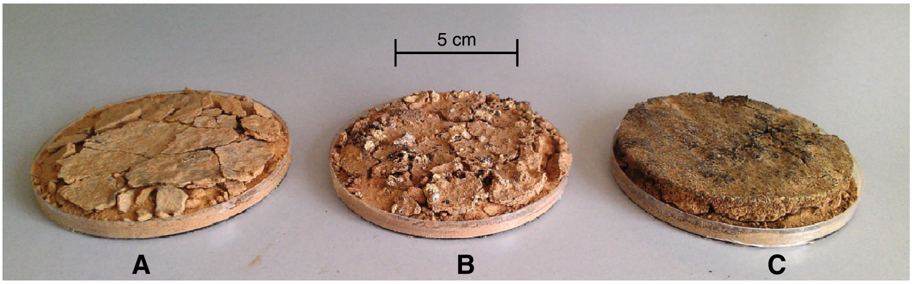

Fig. 3 Biological soil crust samples from three different successional stages. **a** Cyanocrust. **b** Lichencrust. **c** Mosscrust

is described by Lambert–Beer's law (Peth 2010). The attenuation depends on interactions with the atoms of the constituents of the object, namely absorption or a scattering of the beam. At lower energy levels (<150 keV) photoelectric absorption is predominant, which is primarily a function of the effective atomic number and hence material dependent. X-ray attenuation of air is much lower than that of water and solids, thus resulting in a good contrast between the gas and solid/water phase in the tomograms. Attenuation coefficients of different typical soil constituents are provided in Peth (2010). For a detailed description of the use of this technique in soil science, see Peth (2010) and Taina et al. (2008).

Image processing

The reconstructed volumes were manually divided into two regions of interest, the TC and SC by means of the software Visual Studio Max 2.0 (Volume Graphics GmbH, Heidelberg, Germany). The 8-bit grayscale tomograms (Fig. 4a) were segmented using a local thresholding scheme proposed by Oh and Lindquist (1999), which we have found to deliver good results for the binarization of soil pore space (Peth et al. 2008). The method is based on two threshold values in a two-modal grayscale histogram. A Gaussian function was adjusted for each fraction of the histogram, representing solid and pore voxels. Based on the fitted functions two threshold values were defined. Voxels below a lower (T_0) and above an upper (T_1) threshold are classified as definitely pore and solid phase, respectively. Voxels with grayscale values in between the two bounding thresholds (T_0 and T_1) are associated with a high risk for misclassification and marked in the first step as ''uncertain'' voxels. In a second step such "uncertain" voxels are classified based on a short length scale spatial covariance of the image utilizing indicator kriging (Oh and Lindquist 1999). Briefly, the classification of voxels between T_0 and T_1 depends on the voxel grayscale values in their local neighborhood (Fig. 4), from which a probability is calculated for each unclassified voxel to belong to the solid or pore phase using the software 3dma_rock (Lindquist et al. 2005). A more detailed explanation of the application of this procedure in soils can be read in Peth (2010) and Pagenkemper et al. (2013).

Pore features

For the calculation of the pore features, the software MAVI 1.41 (Modular Algorithms for Volume Images, Fraunhofer ITWM, Kaiserslautern) was used. As this program is able to process only rectangular objects, 5 regions of interest of the maximum size possible from each scan were extracted and used as pseudo-replicates for each crust type and depth. The geometric tortuosity of the pores was calculated after skeletonization of the pore network. The algorithm calculated the length of each continuous pore and divided it by the shortest distance between the entrance and exit of that pore, resulting in a number always greater than 1. Total porosity was achieved counting the total number of voxels and multiplying by its volume (166.4 μm^3) using the "field features" algorithm.

The PSD was calculated by means of the "top hat" algorithm implemented in MAVI. This algorithm filled and subsequently counted the pore spaces greater than cubes of twofold and ninefold the minimum voxel size, resulting in 11 and 49.5 μm. These values approximate the equivalent diameter of medium pores (0.2–10 μm), as well as narrow (10–50 μm) and wide (>50 μm) macropores. Due to the scan resolution, part of the medium pores and all of the fine pores (<0.2 μm) could not be detected.

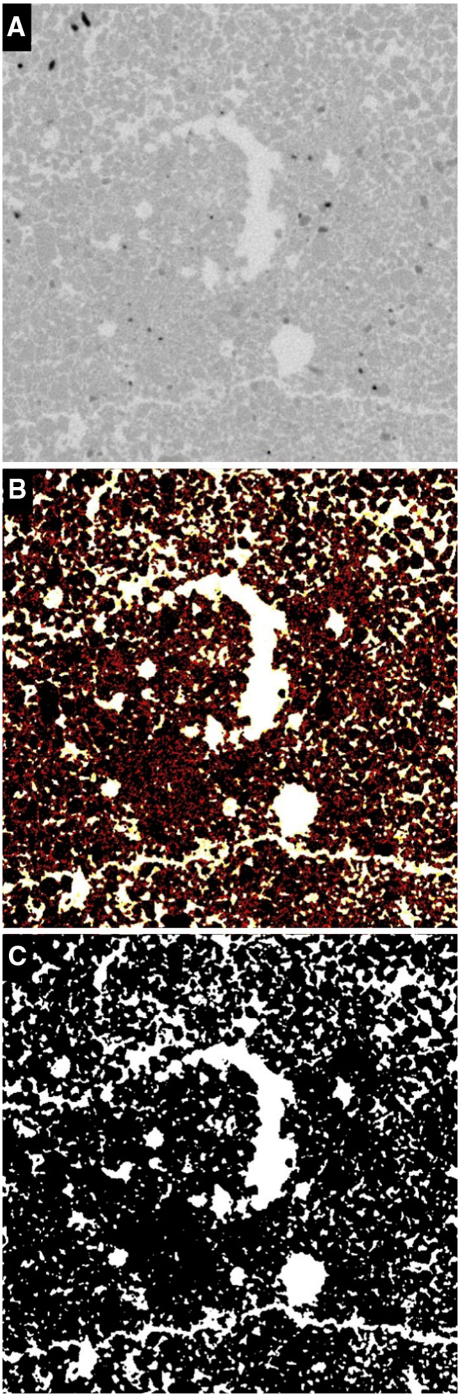

Fig. 4 Scheme of the segmentation process. **a** Original grayscale image from the scan. *Darker* areas denote more dense matter and *lighter* areas denote air. **b** Resulting map of indicator kriging. While the *white* and *black* areas lie above/below the thresholds for pore space and solid phase, the *colored* areas have a higher uncertainty and are interpolated. In this process, *yellow* areas are transformed to pore space and *red* areas to the solid phase. **c** 1-bit *black/white*-image with the *white* areas being the pore space and *black* being the solid phase. (Color figure online)

Thin sections

For thin sections, undisturbed samples of 7 cyanocrusts, 8 lichencrusts and 6 mosscrusts were each impregnated with epoxy resin and then three subsamples were chosen, resulting in 21, 24 and 18 thin sections for each type, respectively. The thin sections ($\sim$20 μm thick) were prepared according to Beckmann (1997) and then analyzed with the optical microscope Keyence VHX 600D. The degree of magnification used varied from 20 to 50× for the macroscopic features and went up to 250–1500× for the microscopic characteristics. All thin sections were analyzed under transmissive and polarized light. The pictures have a resolution of at least 1600 × 1200 pixels.

Bulk density

Bulk Density (BD) of the crusts was measured with a submergence method, using penetrating oil (WD-40, WD-40 Company, San Diego, USA) to saturate the crust and making water penetration impossible. A submergence method was chosen, since it is an easy and fast way for BD determination and is particularly suited for small aggregates (Uteau et al. 2013). Unfortunately, no separation of TC and SC was possible for this method, as the low volume of the TC creates a very high standard deviation.

Statistical analysis

To test the XCMT results for significant differences between each TC and its respective SC, as well as between the same layers of different successional stages, a one-way ANOVA was used. In case of heteroscedasticity, Dunnett's T3 was used and in case of homoscedasticity the Bonferronis test was used as a post hoc test.

Results and discussion

Properties of the pores system

Mercury intrusion porosimetry (MIP)

The results of the MIP are displayed in Table 1 and the PSD is shown in Fig. 5. In accordance with results of Malam Issa et al. (2009), the pore system changes considerably during the succession of BSCs in the NW Negev. Pore sizes measured with MIP should be understood as equivalent diameters of cylindrical pores. However, the slope of the cumulative pressure/volume curve is influenced by the pore shape and therefore, different pore shapes (cylindrical, spherical, rod, plate and needle-like) have different slopes (Webb and Orr 1997). Thus, changes in pore shapes between the different BSCs, which are clearly visible in the XCMT scans (see Fig. 6), are also indicated by the changing cumulative slopes in Fig. 5.

The total porosity of the TC measured with MIP increases in the order CC $<$ LC $<$ MC. The range of pore sizes is higher in the LC and MC, whereas the CC has a more uniform PSD. This is shown by the steeper slope (cumulative graph) as well as the more uniform peak (differential graph) from the CC, as compared to the LC and MC in Fig. 5. As displayed by the high standard deviations, there is a high variation of total porosity as well as pore diameter within all three crust types. Verrecchia et al. (1995) measured a large

Table 1 Porosity of the three biological soil crust types measured by mercury intrusion porosimetry. Numbers in brackets are standard deviations

	Layer	Porosity (%)	Median diameter (μm)
Cyano	TC ($n = 3$)	35.32 (±3.63)	14.39 (±1.77)
	SC ($n = 2$)	50.74 (±5.15)	11.87 (±4.87)
Lichen	TC ($n = 3$)	39.68 (±0.70)	16.22 (±2.77)
	SC ($n = 4$)	37.25 (±5.61)	18.17 (±2.51)
Moss	TC ($n = 3$)	50.13 (±7.53)	25.53 (±3.65)
	SC ($n = 4$)	41.68 (±5.75)	29.48 (±8.52)

number of pores with a diameter between 4 and 40 μm in a CC from Nizzana South. Our results show a dominance of pores between 6 and 60 μm, 3 to 100 μm and 3 to 100 μm for the CC, LC and MC, respectively. The small increase in pores between 3 and 6 μm in the LC and MC can be related to primary pores associated with a higher content of silt and clay. Although Menon et al. (2011) were also able to detect a high variation in porosity, even within the same crust type, their main findings are somewhat different to the ones in this study. While they found decreasing porosities from bare sand to cyanocrusts to cyanobacterial-lichenous crusts in the Kalahari, our data had an opposite trend. However, it can be observed that in the CC the SC has a higher porosity than the topcrust. This relatively high porosity is caused by a vesicular pore system, which is known to be associated with biological or physical soil crusting (Turk and Graham 2011). These vesicles are visible when scraping off the TC of an early stage BSC (Fig. 2e). The abundance of vesicles decreases in the LC (the same pattern was found by Miralles-Mellado et al. 2011), where a slightly higher porosity of the TC compared to the SC was measured. The MC, even though it had the highest variability, exhibited the clearest increase of TC porosity as compared to its respective SC. This is very likely to be caused by the high abundance of mosses that pierce the TC, but do not grow through the entire SC. Along with the increase of total porosity, the median pore diameter increases with crust succession. Here, median pore diameters follow no clear trend between TC and SC, except that they increase with succession caused by the higher abundance of biopores. The higher range of pore sizes in the older crusts is caused by higher amounts of fines, namely silt and clay. This increase of fine particles with crust succession is a common phenomenon in BSCs on sandy soils (Lan et al. 2012; Yair et al. 2011) and caused by the increase of dust trapping efficiency that comes with an increased surface roughness (Reynolds et al. 2001; Williams et al. 2012). Figure 7 illustrates the different dust capture mechanisms of the three crust types in the NW Negev. These fines mainly consist of airborne dust, originating from local wadis and rocky areas of the limestone Negev, as well as from long distance transport of dust from North Africa (Ganor 1991). This causes not only a broader range of pore sizes with crust succession, but also increasing crust thickness and water holding capacity (Yair et al. 2011). Since low porosities and small, unconnected pores are an indicator of low soil quality (Miralles-Mellado et al. 2011; Papadopoulos et al. 2009), the MIP results imply that soil quality increases with crust succession.

XCMT

The results of the XCMT (Table 2) correspond very well to the MIP data and also confirm the change in the pore system with crust succession. The TC shows the same trend of an

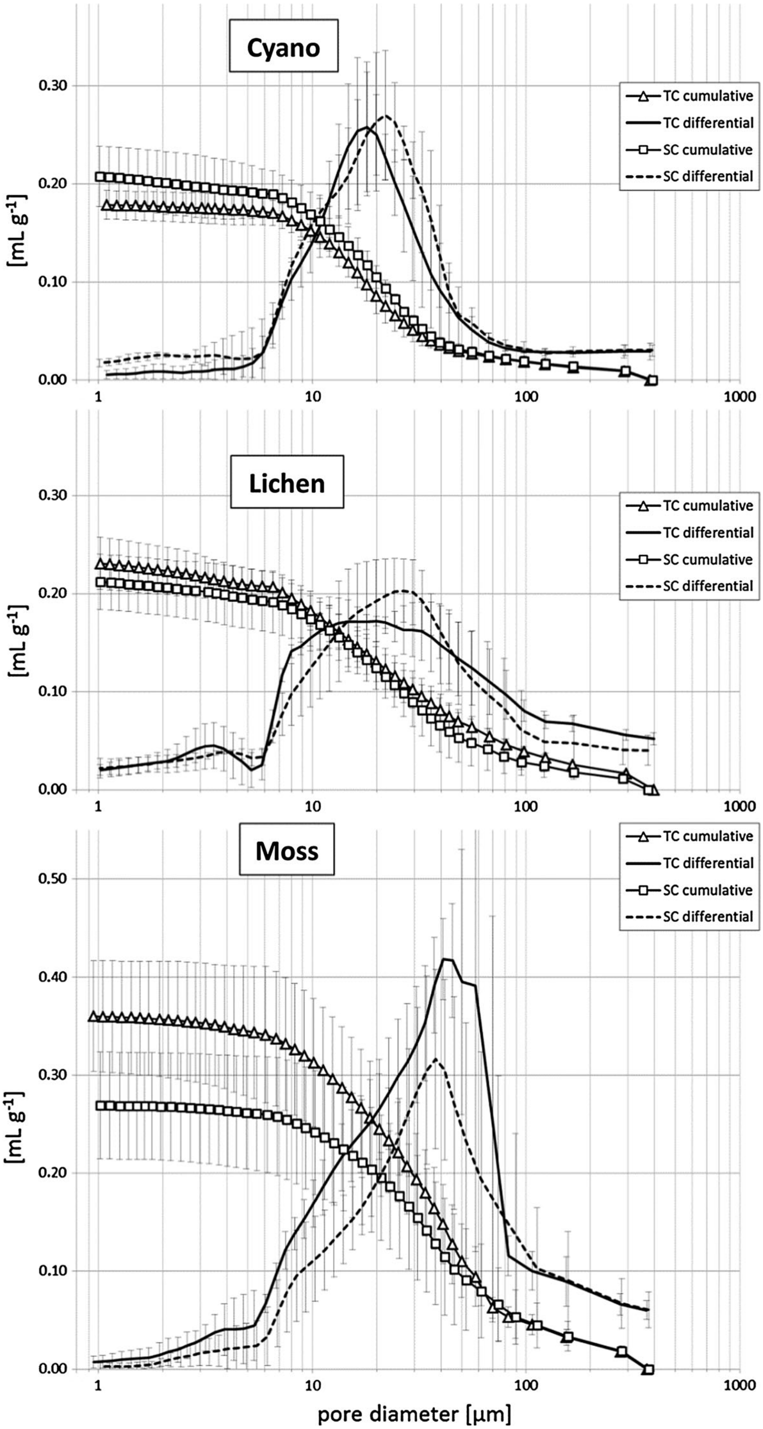

Cyano
0.30
0.20
0.10
0.00
[mL g-1]
1
10
100
1000
TC cumulative
TC differential
SC cumulative
SC differential
Lichen
0.30
0.20
0.10
0.00
[mL g-1]
1
10
100
1000
TC cumulative
TC differential
SC cumulative
SC differential
Moss
0.50
0.40
0.30
0.20
0.10
0.00
[mL g-1]
1
10
100
1000
TC cumulative
TC differential
SC cumulative
SC differential
pore diameter [µm]

◀ **Fig. 5** Cumulative and differential Hg-intrusion *curves* representing the PSD of three types of *top*- and subcrust. *Whiskers* denote standard deviations of 2–4 replicates

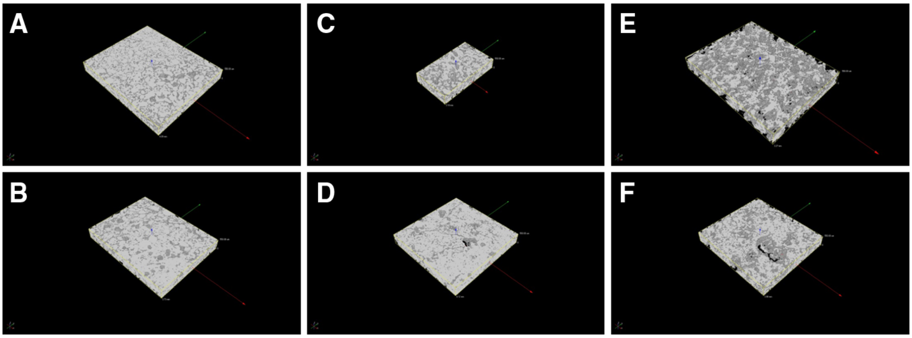

Fig. 6 3D-view of regions of interest of each crust type. For reasons of comparability, each region of interest consists only of 100 slices in the direction of the Z-axis. **a** Topcrust of a cyanocrust with a poorly connected pore system, high tortuosity and some vesicular pores. **b** Subcrust of a cyanocrust with a higher abundance of vesicular pores than in the topcrust. The pore system of this subcrust has the highest tortuosity of all crusts investigated and is therefore poorly connected. **c** Topcrust of a lichencrust with many biogenic macropores and an intermediate tortuosity. **d** Subcrust of a lichencrust, with some large biogenic macropores that reach through the whole region of interest and some shrinkage cracks. **e** Topcrust of a mosscrust, which has the highest porosity and a low tortuosity as compared to the other crusts, caused by the complete perforation of the crust by mosses. **f** Subcrust of a mosscrust. Although the total porosity is somewhat smaller than in its respective topcrust, the pore system of this crust has the lowest tortuosity of all crusts, probably caused by many continuous secondary pores

increasing total porosity during succession, as was detected by MIP. Also, the changes of porosity between TC and SC are in the same magnitude as the ones measured with MIP. While in the CC, the SC has a higher total porosity, the LC and MC show the opposite trend. Only the absolute values are not exactly the same as with MIP because the XCMT method cannot detect pores under 5.5 µm due to the minimum resolution of our scans. The higher porosity in the older crust is partly caused by the increase of organic matter and fines in the crust, but biogenic macro pores, as well as shrinkage cracks, also have a significant impact on the pore system (Fig. 6). These biopores are generated by the growth of stems and rhizoids of bryophytes and rhizines of lichens, as well as the digging activities of small animals in the BSC. This hypothesis is supported also by the results of Eldridge et al. (2010), who found that BSC community structure influences soil microfaunal activity. As indicated in Table 2, the geometric tortuosity of the pore system decreases with succession, indicative of easier water movement through the crust in the later successional stages. The highest tortuosity was measured in the SC of the CC, which is associated with high abundance of unconnected vesicular pores. The differences in tortuosity between TC and SC were significant only in the MC and the decrease of TC tortuosity in the different types was also only significant in the MC, but in the SC the differences were significant between LC and MC, but not CC. The change of the pore structure is also displayed by the change of the three pore size fractions, middle pores (<10 µm), narrow macropores (10–50 µm) and wide macropores (>50 µm). While in the TC of the CC, the relative content of pores >50 µm is very small (1.62 %), it significantly increases to 30.54 % in the SC. This is caused by the increasing abundance of vesicular

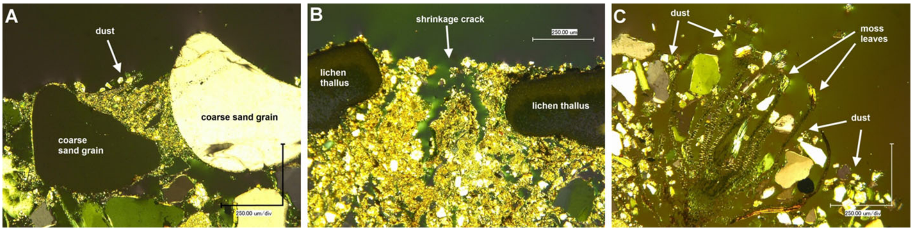

Fig. 7 Thin sections of the surface structure and dust trapping mechanism of different biological soil crusts. **a** The smooth surface of the cyanocrust allows dust to be trapped only between larger sand grains, in this case the *middle* sand fraction. **b** Dust is trapped between the thalli of two lichens (*collema tenax*). The combined shrinking potential of the clays in the dust and the lichen causes initial, small shrinkage cracks to be created between the lichens. **c** The moss leaves capture and trap high amounts of dust, resulting in higher amounts of fines in this BSC type

structures in the SC. With this increase, the content of middle pores and narrow macropores decreases significantly. In the LC, the SC also has a significantly higher content of wide macropores (42.31 %) as compared to its TC (28.47 %), even though the total porosity is significantly higher in the TC than in the SC (33.89 and 25.58 %, respectively). This can be explained by shrinkage cracks and some biogenic macropores caused by roots of annual plants in the SC, which have a higher radius but lower abundance than the pores in the TC (see Fig. 6c, e). The relative percentage of middle pores decreases significantly with crust succession, together with the amount of narrow macropores, while the wide macropores become significantly more abundant. This is why the highest percentage of wide macropores exists in the MC in both TC and SC. Here no significant difference between the pore size fractions could be detected between the layers, which is a result of intensive biogenic mixing. However, the geometric tortuosity and total porosity is significantly higher in the TC. The very low content of pores <10 μm, as well as the very high total porosity that was detected with XCMT, may not fully reflect the true properties of the pore system of the MC. Rather, this is likely to be the result of the loss of some of the very fine silt and clay particles that create these pores and that might have been lost during the segmentation process. This can happen when they are too closely attached to the mosses and therefore have an increased probability of being misinterpreted as pore space when surrounded by voxels, which lie below the threshold for the solid phase, as is the case for the voxels filled with mosses. Although the known underestimation of porosity, which is highest for the smallest pores, lies within the nature of the method due to the limited resolution of the XCMT, it is still the most sophisticated non-destructive way to investigate soil structure, particularly for coarsegrained soils. Moreover, even a moderate resolution can be sufficient when studying the abundance of vesicular pores.

Bulk density

Being negatively correlated with porosity, the change of BD also reflects the change of the pore system during succession. The CC has the highest value of 1.53 ($\pm$0.01) g cm^{-3}, which decreases in the LC to 1.35 ($\pm$0.02) g cm^{-3}, while the MC has the lowest BD with a value of 1.25 ($\pm$0.05) g cm^{-3} ($n = 3$ for all crusts; all differences were significant at $p < 0.05$). The decrease of BD with crust succession is linked to the increase of fines, organic carbon and the abundance of secondary pores and has been reported for BSC around the world. Lan et al. (2012) found a vast decrease in BD from bare sand to

Table 2 Results of the XCMT pore features

Crust Type	Layer	Total Porosity (TP) (%)	Pores >50 µm (% of TP)	Pores 50–10 µm (% of TP)	Pores <10 µm (% of TP)	Tortuosity
Cyano	TC	20.64 (±1.71)[1,a]	1.62 (±1.40)[1,a]	91.62 (±1.21)[1,a]	6.76 (±0.62)[1,a]	1.48 (±0.07)[1,a]
	SC	26.11 (±3.41)[2,a]	30.54 (±10.12)[2,a]	65.45 (±9.42)[2,a]	4.00 (±0.87)[2,a]	1.63 (±0.45)[1,a]
Lichen	TC	33.89 (±2.58)[1,b]	28.47 (±4.05)[1,b]	68.62 (±3.88)[1,b]	2.91 (±0.25)[1,b]	1.36 (±0.05)[1,a]
	SC	25.58 (±2.12)[2,ab]	42.31 (±8.59)[2,a]	54.45 (±8.25)[2,a]	3.24 (±0.43)[1,a]	1.36 (±0.07)[1,ab]
Moss	TC	62.25 (±1.98)[1,c]	64.12 (±4.84)[1,c]	34.57 (±4.63)[1,c]	1.31 (±0.24)[1,c]	1.22 (±0.02)[1,b]
	SC	49.93 (±2.19)[2,bc]	60.57 (±2.67)[1,b]	37.73 (±2.60)[1,b]	1.69 (±0.14)[1,b]	1.17 (±0.01)[2,ac]

TP Total porosity, tortuosity and relative percentage of pore size fractions (% of TP) of the crust. Different numbers denote significant differences between the respective other layer. Different letters denote significant differences to the same layer of other successional stages. Differences are significant at $p < 0.05$

algaecrusts to lichencrusts to mosscrusts. The values measured in the Shapotou Region, China dropped from 1.81 to 1.04 g cm^{-3}, which is a much higher difference than the one we found for the NW Negev. The change of BD with crust development can not only be observed for the crust itself, but also for the topsoil underlying the BSC. Guo et al. (2008) found in Inner Mongolia linearly decreasing BD values from soils under physical crusts, to soils under lichencrusts and soils under mosscrusts. Since soil porosity is a good indicator for soil quality (Miralles-Mellado et al. 2011; Papadopoulos et al. 2009), it can be stated that with ongoing succession of BSCs, the soil quality in terms of the pore system increases not only for the BSC but also for the topsoil directly underneath it.

Structure

The structural analysis of the XCMT scans and the thin sections is described below.

Surface

In general, the surface roughness increases with succession (Rodríguez-Caballero et al. 2012; Williams et al. 2012). In the CC, a very even and smooth surface can be observed (Figs. 2c and 7a), resulting in a high connectivity of runoff paths, whereas the lichen thalli in the LC have an uneven surface and create shrinkage cracks in which dust can accumulate (Fig. 7b). The moss leaves in the MC also highly increase surface roughness and along with it dust trapping efficiency (Fig. 7c). This increase in dust trapping efficiency results in a much higher content of silt and clay (Almog and Yair 2007), which in turn increases the shrink-swell potential of the topcrust. A detailed description of the mechanisms leading to the complex micro-topography of BSCs in arid environments is given by Williams et al. (2012).

Pore continuity

While a clear vertical stratification of altering layers of fine and coarse material is visible in the CC, this layering becomes weaker during succession due to increased biological activity. In the early stage CC, only the TC layer is enriched in fines and shows no pathways for preferential infiltration, such as biopores and shrinkage cracks. As succession continues, the amount and distribution of fines increases due to increased dust trapping and

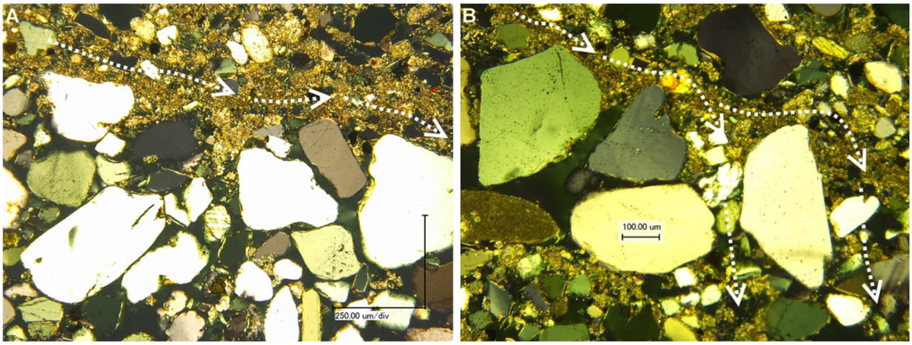

Fig. 8 **a** Finegrained layer over a coarsegrained layer. Capillary barrier occurs at the interface of the two layers. **b** Discontinuous pores on the *left* side of the image with a sharp border between the coarse and fine grains. A continuous pore space on the right side of the image, where fines are washed into the interspace of larger grains. *Dotted white arrows* denote potential water movement path

microscale mass wasting (cf. Williams et al. 2012). Some crusts, particularly the ones existing in small depressions or in the leeside of shrub mounds, where wind speeds are low and sand is deposited after a sandstorm, not only have one TC and SC, but different layers of relict TCs. These areas of higher fine content reflect a former TC that got buried by larger sand grains during a sand storm. Due to the reduction of light and available moisture, the microorganisms that were buried then migrated to the new soil surface (Garcia-Pichel and Pringault 2001) where new dust had accumulated, which again increased the water holding capacity at the surface. As soon as these organisms found themselves in an environment that allowed metabolic activity due to the presence of light and water, they formed a new TC through the excretion of extracellular polymeric substances (EPS). This sequence can repeat itself several times such that multiple layers of this kind can form (Fig. 2d). The change of relatively large and very small particles in the crust can be partly responsible for impeded infiltration through the crust due to the occurrence of a capillary barrier effect that is caused by the discontinuity of the pore space. This effect describes a situation when there is a sharp border between relatively small pores and relatively large ones (Fig. 8a). As long as the capillary forces of the water are stronger than the hydrostatic pressure that is applied by the water layer that rests on top of the capillary barrier, no infiltration will take place. This impeded water movement leads to rapid saturation of the upper finegrained layer, resulting in a strong local increase of hydraulic conductivity. In the case of an inclination of the system, it leads to a lateral diversion instead of vertical infiltration of the water (Zornberg et al. 2010). The lateral diversion capacity of this mechanism on the large scale is determined by several variables: (i) the steeper the slope, the faster the water is transported laterally, (ii) the longer the slope, the more water will accumulate at the base, increasing the hydrostatic pressure on the water menisci and eventually causing the effect to breakdown (Morris and Stormont 1999), and (iii) the more homogeneous the grains are distributed (i.e. the more distinct the border between the layers), the higher the efficiency of the mechanism since no areas of preferential infiltration (fingering) will occur (Ho and Webb 1998; Steenhuis et al. 2005). Especially due to the vast heterogeneity of grain size distributions within the BSC, it seems unlikely that this mechanism has great influence on water movement at the large scale. Still, on a very small scale, it can account for at least some of the restraint infiltration. The very dimension of this small scale becomes evident in Fig. 8b, where the transition from a discontinuous to a continuous pore space occurs over a distance of only 1–2 mm. Also, this mechanism is able to explain the fact that runoff in the NW Negev was predominantly observed on pre-wetted crusts. This is because with the first small rain event of only a few mm, all the capillary breaks at the interface are filled with water and a saturation of the finegrained layer can already take place. With the next small rain event, runoff can start immediately when the raindrops touch the soil surface. This is especially true when the crust was pre-wetted by dew, which was shown to be a very frequent phenomenon in the NW Negev (Jacobs et al. 2000). Furthermore, this casts doubt on the explanation of the pore clogging effect as being primarily responsible for a decrease of hydraulic conductivity after wetting, as reported by Fischer et al. (2010) and Kidron et al. (1999).

Vesicular pores

The abundance of vesicular structures in the NW Negev crusts decreases with succession. While in the young CC even the existence of small micro-vesicular horizons can be observed (Fig. 2d, f), the abundance of these structures decreases towards the LC and even more towards the MC, where hardly any such pores are present. Vesicular pores are formed when air is trapped in the soil due to a migrating wetting front that seals the surface. The following increase of gas pressure and reduction of inter-grain connection ultimately leads to the creation of spherical, unconnected voids in the soil matrix (Dietze et al. 2012; Springer 1958). According to Evenari et al. (1974), this process requires surface sealing by either a mineral or a biological crust. Turk and Graham (2011) named three factors required for the growth of vesicular horizons, namely the addition of eolian material, the development of a surface seal in the form of an embedded gravel layer (desert pavement) or a physical or a biological crust and wet-dry cycles. Dietze et al. (2012), however, were able to show that surface sealing in the form of a crust is not necessarily required for the formation of vesicles, but did not exclude the possibility of them being influenced by it. Yonovitz and Drohan (2009) for example found vesicular horizons as thick as 9 mm under mineral and BSCs and Turk and Graham (2011) stated that due to their higher dust trapping efficiency, caused by higher surface roughness, BSCs of later successional stages or from colder deserts have a positive impact on the formation of vesicular structures. This is also confirmed by Williams et al. (2012), who described a model of vesicular horizon formation under BSCs. Our results, however, show a clear decrease of such structures during succession within the BSCs, which agrees with the results of Miralles-Mellado et al. (2011), who found vesicular pores in incipient BSCs but not in lichencrusts, where large, elongated pores predominated. This means that the increased dust trapping can only influence vesicular horizons underneath the BSCs, which lie out of range of the BSC-induced bioturbation. In laboratory experiments, both Dietze et al. (2012) and Figueira and Stoops (1983) were able to create vesicular structures after 5 wet–dry cycles, indicating that a similar quantity of rain events is at least necessary for vesicles to develop in situ. This quick development of vesicular porosity in the field is also confirmed by Yonovitz and Drohan (2009), who found a vesicular horizon re-developing in the Mojave Desert (USA) only 1 month after its destruction by mechanical disturbance. The position by Springer (1958), that vesicular structures are an unstable and transitory condition in pedogenetic processes and that the pores are destroyed after each wet-dry cycle, was disproved by Dietze et al. (2012), who found vesicles to be stable, unless deliberately destroyed. Destruction is, however, very likely to happen when bioturbation by soil flora and fauna causes a rearrangement of soil particles. Since the strongest natural antagonistic mechanism of vesicular structures is root growth (Dietze et al. 2012), it can be assumed that the

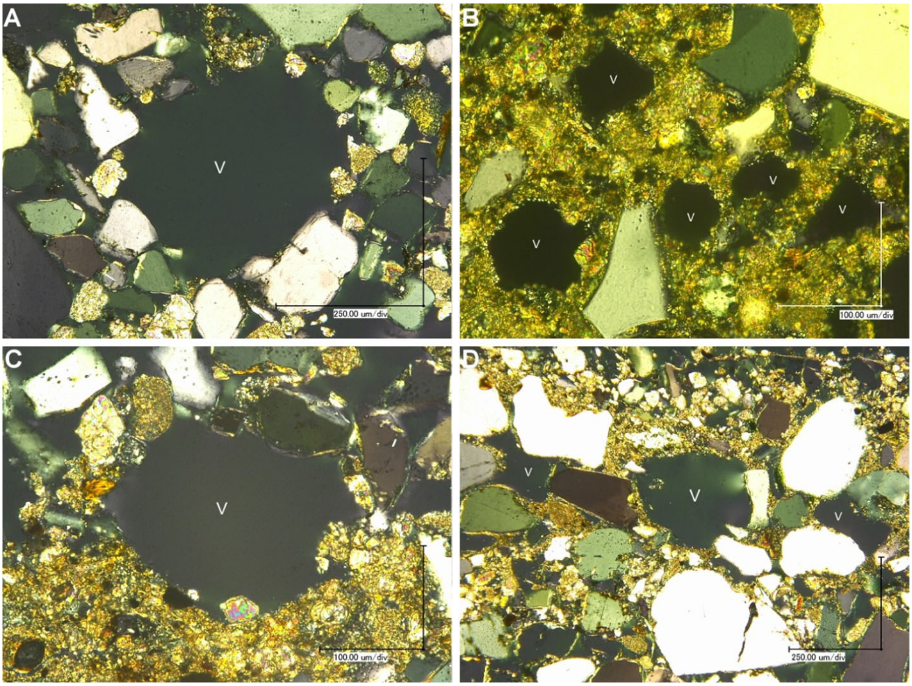

Fig. 9 Vesicular pores (V) in various depths of a cyanocrust. **a** A single, spherical vesicular pore that formed in a coarsegrained layer. This pore is not completely disconnected from the rest of the pore space and will, to a certain degree, take part in water movement. **b** Multiple vesicular pores of various forms that formed in a finegrained layer. These vesicles are completely isolated and non-connective. The soil volume occupied by such structures is not accessible for infiltration. **c** Semi-spherical vesicular pore that formed precisely at the interface between a coarse and a finegrained layer. **d** Non-spherical vesicular pores in a layer with mixed grain sizes

decreasing abundance of vesicles with crust succession is caused by (i) active destruction by the rhizoids and rhizines of lichen and mosses, and (ii) the existence of secondary pores that run through the whole crust, inhibiting surface sealing by a wetting front after a rain event, thereby preventing vesicle formation (Dietze et al. 2012). Furthermore, Dietze et al. (2012) found a negative correlation between vesicle size and carbonate content, which they attribute to the small size and thus the higher particle cohesion of the carbonates in their experiment. On the other hand, the sand content was positively correlated with vesicle size. In accordance with these findings, Fig. 9 displays the various shapes of vesicular pores in crusts from the NW Negev. Vesicles are abundant in both finegrained and coarsegrained layers and even on the interface between them. Figure 9a shows a single, large, spherical vesicle in a coarsegrained layer, while Fig. 9b shows multiple small, spherical and non–connected vesicles in a finegrained layer rich in carbonates. The fact that vesicles are frequently found in the CC in various depths (even on the interface between fine- and coarsegrained layers, as shown in Fig. 9c) and with no obvious correlation to the grain size highlights the importance of the advancing wetting front, which determines the location of vesicle formation in the upper cm of the soil profile. The non-sphericity of some of the vesicular pores in Fig. 9d is a result of the high content of coarse sand grains and the relatively low silt content.

Due to the fact that vesicular horizons have been reported to decrease drastically the infiltration capacity ({Young 2004 #391}), it is very probable that they also have an impeding effect on water infiltration on the BSCs in the NW Negev. This is because these kinds of pores are mostly spherical, well rounded and mainly non-connected. This poor connectivity is the reason why they do not take part in the infiltration process. Dietze et al. (2012) found the infiltration capacity of artificial vesicular horizons to decrease significantly on a logarithmical scale with ongoing vesicle formation. Although Blume et al. (2008) described vesicular structures in the NW Negev, they only referred to the upper cm of the salty playa soils, devoid of BSCs, and to the SC of BSC in an adjacent interdune, but not for the slope positions. Since that study took place in the late 1990s, the conditions presumably have changed in the meantime and vesicles have become more abundant along the entire dune relief. Because it is particularly the slope positions, where vesicular structures have the highest influence on water redistribution and runoff generation, it can be assumed that if these structures formed only within the last 15–20 years, there has also been an accompanying shift in factors determining runoff generation. Because vesicle formation is mainly a physical, rather than biological mechanism (Dietze et al. 2012) and since vesicular structures were also found in the playa of the southernmost study site (Blume et al. 2008) that lacked BSC, we believe that even though vesicles might also exist in the NW Negev without BSCs and vice versa, they do reinforce the redistribution of water caused by BSCs. In this way, they accelerate the development of the BSCs and are likely to be responsible for a faster succession of BSCs in run-on areas as compared to areas devoid of vesicular structures. Although we describe only the situation of the NW Negev, it is probable that similar mechanisms determine the impact that BSCs have on hydrological processes worldwide, under similar environmental conditions.

Synthesis and conclusions

Because of higher contents of fines and organic matter, BSCs are considered a physical discontinuity in the soil profile, which alters the hydrological properties of the soil in the uppermost centimeters (Coppola et al. 2011). We have pointed out that, depending on the successional stage and the type of SC, this discontinuity exists not only between soil and respective crust but also within the crust itself, namely between TC and SC, and that it becomes weaker as succession continues. We conclude that the influences of the structural properties of BSCs must be considered to a much greater extent when investigating their hydrological behavior. We propose two new mechanisms for the explanation of the high runoff values on smooth, cyanobacterial BSCs in the NW Negev. These are (i) the vesicular porosity within the crust that strongly limits infiltration, and (ii) the capillary barrier effect, that develops wherever a change in pore sizes takes place and is caused when coarse sand grains are deposited over finegrained dust at high wind speeds during a sand storm. We suggest that the importance of swelling of both biological and mineral components of the BSC and the subsequent clogging of pores might have been overestimated in previous research (Fischer et al. 2010; Kidron et al. 1999; Verrecchia et al. 1995), whereas the influence of soil microstructure (i.e. the structure of the pore system) has been underestimated. Yet since in soils there is no single cause for a specific phenomenon, the real reason for runoff at the landscape scale might be a complex interaction between many mechanisms, whose intensities and combination are constantly changing on a very small scale. This means that at the smallest scale, local conditions might have great variations over very small distances. In one spot, where vesicles are absent, a capillary barrier effect might reduce the infiltration of water but on a neighboring spot where vesicles are dominant, the vesicles will impede infiltration. Where neither of these is present, it might be hydrophobicity, which mainly influences water movement.

This qualitative description of the internal BSC microstructure represents an important step forwards in understanding the hydrological properties of BSCs. Further research should focus on a quantitative investigation of the abundance of vesicular structures in the field, combined with a modeling of water movement in the BSC using XCMT techniques and also taking into account the continuity of the pore system. Only in this way can the real contribution of these phenomena be determined for runoff generation in the NW Negev dunes.

Acknowledgments We thank the German Research Foundation (Deutsche Forschungsgemeinschaft) for funding this research in the framework of their Trilateral Project "Biotic and abiotic factor affecting biological soil crust formation and recovery in a semiarid dune ecosystem, Gaza and NW Negev" (Project FE 218/14-2), and the Arid Ecosystems Research Center of the Hebrew University of Jerusalem for access to their field sites. Special thanks are due to Simon Berkowicz for his great support during fieldwork and for editing. We also thank the team of the Institute of Plant Nutrition and Soil Science of the University of Kiel for their help during the XCMT analyses.

References

Almog R, Yair A (2007) Negative and positive effects of topsoil biological crusts on water availability along a rainfall gradient in a sandy arid area. Catena 70(3):437–442

Beckmann T (1997) Preparation of soil thin sections for micromorphological research. In: Hohenheimer bodenkundliche hefte. Mikromophologische Methoden in der Bodenkunde, pp89–103

Belnap J (2002) Nitrogen fixation in biological soil crusts from southeast Utah, USA. Biol Fertil Soils 35:128–135

Belnap J (2006) The potential roles of biological soil crusts in dryland hydrologic cycles. Hydrol Process 20(15):3159–3178

Belnap J, Gillette DA (1998) Vulnerability of desert biological soil crusts to wind erosion: the influences of crust development, soil texture, and disturbance. J Arid Environ 39:133–142

Berkeley A, Thomas AD, Dougill AJ (2005) Cyanobacterial soil crusts and woody shrub canopies in Kalahari rangelands. African J Ecol 43(2):137–145

Blume H, Beyer L, Pfisterer U et al (2008) Soil characteristics and pattern of the Nizzana research site. In: Breckle S, Yair A, Veste M (eds) Arid dune ecosystems. The Nizzana sands in the Negev Desert Springer, Berlin, pp 65–77 1 online resource (xxvi, 475

Büdel B, Veste M (2008) Biological crusts. In: Yair A, Veste M (eds) Arid dune ecosystems. The Nizzana sands in the Negev Desert Springer, Berlin, pp 149–155 1 online resource (xxvi, 475

Chamizo S, Cantón Y, Rodríguez-Caballero E et al (2012) Runoff at contrasting scales in a semiarid ecosystem: a complex balance between biological soil crust features and rainfall characteristics. J Hydrol 452–453:130–138

Coppola A, Basile A, Wang X et al (2011) Hydrological behaviour of microbiotic crusts on sand dunes: example from NW China comparing infiltration in crusted and crust-removed soil. Soil Tillage Res 117:34–43

Darby BJ, Neher DJ, Belnap J (2010) Impact of biological soil crusts and desert plants on soil microfaunal community composition. Plant Soil 328:421–431

Delgado-Baquerizo M, Morillas L, Maestre FT et al (2013) Biocrusts control the nitrogen dynamics and microbial functional diversity of semi-arid soils in response to nutrient additions. Plant Soil 372:643–654

Dietze M, Bartel S, Lindner M et al (2012) Formation mechanisms and control factors of vesicular soil structure. Catena 99:83–96

Drahorad SL, Felix-Henningsen P (2012) An electronic micropenetrometer (EMP) for field measurements of biological soil crust stability. Z. Pflanzenernähr. Bodenk. 175(4):519–520

Drahorad SL, Felix-Henningsen P (2013) Application of an electronic micropenetrometer to assess mechanical stability of biological soil crusts. J Plant Nutr Soil Sci:n/a 176:904–909

Drahorad SL, Felix-Henningsen P, Eckhardt K et al (2013) Spatial carbon and nitrogen distribution and organic matter characteristics of biological soil crusts in the Negev desert (Israel) along a rainfall gradient. J Arid Environ 94:18–26
Eldridge DJ, Bowker MA, Maestre FT et al (2010) Interactive effects of three ecosystem engineers on infiltration in a semi-arid mediterranean Grassland. Ecosystems 13(4):499–510
Evenari M, Yaalon DH, Guttermann Y (1974) Note on soils with vesicular structure in deserts. Z für Geomorphol 18:162–172
Felix-Henningsen P, Rummel B, Blume H (2008) Soil processes and salt dynamics in dune soils. In: Breckle S, Yair A, Veste M (eds) Arid dune ecosystems. The Nizzana sands in the Negev Desert Springer, Berlin, pp 225–238 1 online resource (xxvi, 475
Ferreiro JP, Miranda JGV, Vazquez EV (2010) Multifractal analysis of soil porosity based on mercury injection and nitrogen adsorption. Vadose Zone J 9:325–335
Figueira H, Stoops G (1983) Application of micromorphometric techniques to the experimental study of vesicular layer formation. Pedologie 33(1):77–89
Fischer T, Veste M, Wiehe W et al (2010) Water repellency and pore clogging at early successional stages of microbiotic crusts on inland dunes, Brandenburg, NE Germany. Catena 80:47–52
Ganor E (1991) The composition of clay minerals transported to israel as indicators of saharan dust emission. Atmos Environ 25(12):2657–2664
Garcia-Pichel F, Pringault O (2001) Cyanobacteria track water in desert soils. Nature 413:380–381
Guo Y, Zhao H, Zuo X et al (2008) Biological soil crust development and its topsoil properties in the process of dune stabilization, Inner Mongolia, China. Environ Geol 54:653–662
Hernandez RR, Sandquist DR (2011) Disturbance of biological soil crust increases emergence of exotic vascular plants in California sage scrub. Plant Ecol 212(10):1709–1721
Ho CK, Webb SW (1998) Capillary barrier performance in heterogeneous porous media. Water Resour Res 34(4):603–609
Hu C, Zhang D, Huang Z et al (2003) The vertical microdistribution of cyanobacteria and green algae within desert crusts and the development of the algal crusts. Plant Soil 257(1):97–111
Jacobs AFG, Heusinkveld BG, Berkowicz SM (2000) Dew measurements along a longitudinal sand dune transect, Negev Desert, Israel. Int J Biometeorol 43:184–190
Kidron GJ, Yair A (1997) Rainfall-runoff relationship over encrusted dune surfaces, Nizzana, Western Negev, Israel. Earth Surf Proc Land 22:1169–1184
Kidron GJ, Yaalon DH, Vonshak A (1999) Two causes for runoff initiation on microbiotic crusts: hydrophobicity and pore clogging. Soil Sci 164(1):18–27
Kidron GJ, Vonshak A, Dor I et al (2010) Properties and spatial distribution of microbiotic crusts in the Negev Desert, Israel. Catena 82:92–101
Kidron GJ, Monger HC, Vonshak A et al (2012) Contrasting effects of microbiotic crusts on runoff in desert surfaces. Geomorphology 139–140:484–494
Lan S, Wu L, Zhang D et al (2012) Successional stages of biological soil crusts and their microstructure variability in Shapotou region (China). Environ Earth Sci 65(1):77–88
Lichner L, Hallett PD, Drongová Z et al (2013) Algae influence the hydrophysical parameters of a sandy soil. Catena 108:58–68
Lindquist B, Lee S, Oh W et al (2005) 3DMA-Rock: A software package for automated analysis of rock pore structure in 3-D computed microtomography images. http://www.ams.sunysb.edu/~lindquis/3dma/3dma_rock/3dma_rock.html#Sec_Intro. Accessed 14 Nov 2013
Littmann T, Berkowicz SM (2008) The regional climatic setting. In: Breckle S, Yair A, Veste M (eds) Arid dune ecosystems. The Nizzana sands in the Negev Desert Springer, Berlin, pp 49–63 1 online resource (xxvi, 475
Liu Y, Li X, Jia R et al (2011) Effects of biological soil crusts on soil nematode communities following dune stabilization in the Tengger Desert, Northern China. Appl Soil Ecol 49:118–124
Mager DM (2010) Carbohydrates in cyanobacterial soil crusts as a source of carbon in the southwest Kalahari. Soil Biol Biochem 42(2):313–318
Malam Issa O, Défarge C, Trichet J et al (2009) Microbiotic soil crusts in the Sahel of Western Niger and their influence on soil porosity and water dynamics. Catena 77(1):48–55
Malam Issa O, Valentin C, Rajot JL et al (2011) Runoff generation fostered by physical and biological crusts in semi-arid sandy soils. Geoderma 167–168:22–29
Menon M, Yuan Q, Jia X et al (2011) Assessment of physical and hydrological properties of biological soil crusts using X-ray microtomography and modelling. J Hydrol 397:47–54
Miralles-Mellado I, Cantón Y, Solé-Benet A (2011) Two-dimensional porosity of crusted silty soils: indicators of soil quality in semiarid rangelands? Soil Sci Soc Am J 75(4):1330

Morris CE, Stormont JC (1999) Parametric study of unsaturated drainage layers in a capillary barrier. J Geotech Geoenviron Eng 125(12):1057–1065
Oh W, Lindquist B (1999) Image thresholding by indicator kriging. IEEE Trans Pattern Anal Mach Intell 21(7):590–602
Pagenkemper SK, Peth S, Uteau D (2013) Effects of root-induced biopore architectures on physical processes investigated with industrial X-ray computed tomography. In: Anderson SH, Hopmans JW et al (eds) Tomography and imaging of soil–water–root processes, 2nd edn. SSSA Special Publication, Madison, pp 69–96
Papadopoulos A, Whitmore AP, White RP et al (2009) Combining spatial resolutions in the multiscale analysis of soil pore-size distributions. Vadose Zone J 8(1):227
Peth S (2010) Applications of microtomography in soils and sediments. In: Singh B, Gräfe M (eds) Synchrotron-based techniques in soils and sediments. Elsevier, Amsterdam, pp 73–101 1 online resource (1 recurs electrònic (vii, 480
Peth S, Horn R, Beckmann F et al (2008) Three-dimensional quantification of intra-aggregate pore-space features using synchrotron-radiation-based microtomography. Soil Sci Soc Am J 72(4):897
Prasse R, Bornkamm R (2000) Effect of microbiotic soil surface crusts on emergence of vascular plants. Plant Ecol 150:65–75
Reynolds RL, Belnap J, Reheis MC et al (2001) Aeolian dust in Colorado Plateau soils: nutrient inputs and recent change in source. Proc Natl Acad Sci 98(13):7123–7127
Rodríguez-Caballero E, Cantón Y, Chamizo S et al (2012) Effects of biological soil crusts on surface roughness and implications for runoff and erosion. Geomorphology 145–146:81–89
Rossi F, Potrafka RM, Garcia-Pichel F et al (2012) The role of the exopolysaccharides in enhancing hydraulic conductivity of biological soil crusts. Soil Biol Biochem 46:33–40
Rummel B, Felix-Henningsen P (2004) Soil water balance of an arid linear sand dune. Int Agrophys 18:333–337
Springer ME (1958) Desert pavement and vesicular layer of some soils of the desert of the Lahontan Basin, Nevada1. Soil Sci Soc Am J 22(1):63–66
Steenhuis TS, Parlange J, Kim Y et al (2005) Unstable flow. In: Hillel D (ed) Encyclopedia of soils in the environment, vol 4. Elsevier Academic Press, Amsterdam, pp 197–201
Su Y, Li XR, Zheng J et al (2009) The effect of biological soil crusts of different successional stages and conditions on the germination of seeds of three desert plants. J Arid Environ 73(10):931–936
Taina IA, Heck RJ, Elliot TR (2008) Application of X-ray computed tomography to soil science: a literature review. Can J Soil Sci 88(1):1–19
Tsoar H (2008) Land use and its effect on the mobilization and stabilization of the north-western Negev sand dunes. In: Breckle S, Yair A, Veste M (eds) Arid dune ecosystems. The Nizzana sands in the Negev Desert Springer, Berlin, pp 79–89 1 online resource (xxvi, 475)
Turk JK, Graham RC (2011) Distribution and properties of vesicular horizons in the western United States. Soil Sci Soc Am J 75(4):1449–1461//1449
Uteau D, Pagenkemper SK, Peth S et al (2013) Aggregate and soil clod volume measurement: a method comparison. Soil Sci Soc Am J 77(1):60
Valentin C, Bresson L (1992) Morphology, genesis and classification of surface crusts in loamy and sandy soils. Geoderma 55:225–245
Verrecchia E, Yair A, Kidron GJ et al (1995) Physical properties of the psammophile cryptogamic crust and their consequences to the water regime of sandy soils, north-western Negev Desert, Israel. J Arid Environ 29:427–437
Webb P, Orr C (1997) Analytical methods in fine particle technology. Micromeritics Instrument Corp, Norcross, Ga
Williams AJ, Buck BJ, Beyene MA (2012) Biological soil crusts in the Mojave Desert, USA: micromorphology and pedogenesis. Soil Sci Soc Am J 76(5):1685
Yair A (1990) Runoff generation in a sandy area—the nizzana sands, Western Negev, Israel. Earth Surf Proc Land 15:597–609
Yair A, Almog R, Veste M (2011) Differential hydrological response of biological topsoil crusts along a rainfall gradient in a sandy arid area: northern Negev desert, Israel. Catena 87:326–333
Yonovitz M, Drohan PJ (2009) Pore morphology characteristics of vesicular horizons in undisturbed and disturbed arid soils; implications for arid land management. Soil Use Manag 25(3):293–302
Zhang Y, Wang H, Wang X et al (2006) The microstructure of microbiotic crust and its influence on wind erosion for a sandy soil surface in the Gurbantunggut Desert of Northwestern China. Geoderma 132(3–4):441–449
Zornberg J, McCartney J, Bouazza A (2010) Geosynthetic capillary barriers: current state of knowledge. Geosynth Int 17(5):273–300